RESULTS OF SPACE DEBRIS SURVEY OBSERVATIONS ON HIGHLY-ECCENTRIC MEO ORBITS

Andreas Hinze[(1)(2)], T. Schildknecht[(2)], T. Flohrer[(3)], H. Krag[(3)]

[(1)] DLR, Münchner Strasse 20, 82234 Wessling, Germany, andreas.hinze@dlr.de
[(2)] Astronomical Institute, University of Bern, Switzerland, Sidlerstrasse 5, 3012 Bern, thomas.schildknecht@aiub.unibe.ch
[(3)] ESA/ESOC , Robert-Bosch-Str. 5, 64293 Darmstadt, (holger.krag; tim.flohrer)@esa.int

ABSTRACT

Optical surveys for space debris in high-altitude orbits have been conducted since more than ten years. First observation strategies and processing techniques were successfully developed for the geostationary ring (GEO). The observations scenarios were adjusted for observations in the geostationary transfer orbit (GTO) and in the medium Earth orbit (MEO).

After the already investigated circular MEO orbits of the GPS and GLONASS constellations the Astronomical Institute of the University of Bern (AIUB) developed survey and follow-up strategies for the systematically search of space debris in highly-eccentric orbits in the MEO region, in particular in Molniya-type orbits. Several breakup events and deliberate fragmentations are known to have taken place in such orbits. The AIUB performed several survey campaigns between January 2013 and April 2013 to search for debris objects in this MEO region. The optical observations were conducted in the framework of an ESA study using ESA's Space Debris Telescope (ESASDT) the 1-m Zeiss telescope located at the Optical Ground Station (OGS) at the Teide Observatory at Tenerife, Spain. The results from the different observation campaigns will be presented.

1 INTRODUCTION

The space debris environment in the MEO region was rarely systematically investigated so far. Recently, an extension of the ongoing space debris surveys to new orbital regions, in particular to the increasingly populated medium Earth orbit (MEO) region was undertaken. In this latter study the work focused on circular MEO orbits including GPS and GLONASS constellations [1], [2].

The highly-eccentric MEO orbits investigated in this work include in particular Molniya orbits with an inclination of about 63.4°, an argument of perigee of about -90°, and a revolution period of one half of a sidereal day. With an eccentricity around 0.7 and apogee altitudes around 40.000km, the orbits are conceived such that a spacecraft would spend a considerable period of time around apogee over the northern hemisphere. The 63.4° inclination is chosen to minimize the secular perturbation of the argument of perigee caused by the Earth´s oblateness.

2 POPULATION

In order to the current population in the selected orbital region we used the following limits to select objects from the USSTRATCOM catalogue of unclassified objects (January 2012):

$$60° < i < 67°$$

$$0.5 < e < 0.8$$

$$20000\text{km} < a < 30000\text{km}$$

A semi major axis between 20000km and 30000km corresponds to a mean motion of about 2 revolutions per day. We set no limit in right ascension of the ascending node (RAAN) and for the argument of the perigee. Finally 171 objects (Table 1) in the USSTRATCOM catalogue fulfilled the above criteria (also called TLE population).

Table 1: Objects of the the TLE population in Molniya orbit region (USSTRATCOM catalogue January 2012).

Description	Quantity
MOLNIYA satellites	41
Rocket bodies	73
Others	57
Total	171

Figure 1 shows the distribution of the orbital elements of the selected TLE population. The nodes are distributed over the whole range of right ascension with a concentration between 0° and 200°. The inclinations are concentrated around the nominal value of 63.4° (critical inclination). Based on the distribution of the eccentricity it was possible to separate a subgroup consisting of 35 objects including rocket bodies (10), debris (20) and OKO satellites (5) with an eccentricity of less than 0.65. These objects form a group with similar orbital elements and launch date.

Proc. '6th European Conference on Space Debris'
Darmstadt, Germany, 22–25 April 2013 (ESA SP-723, August 2013)

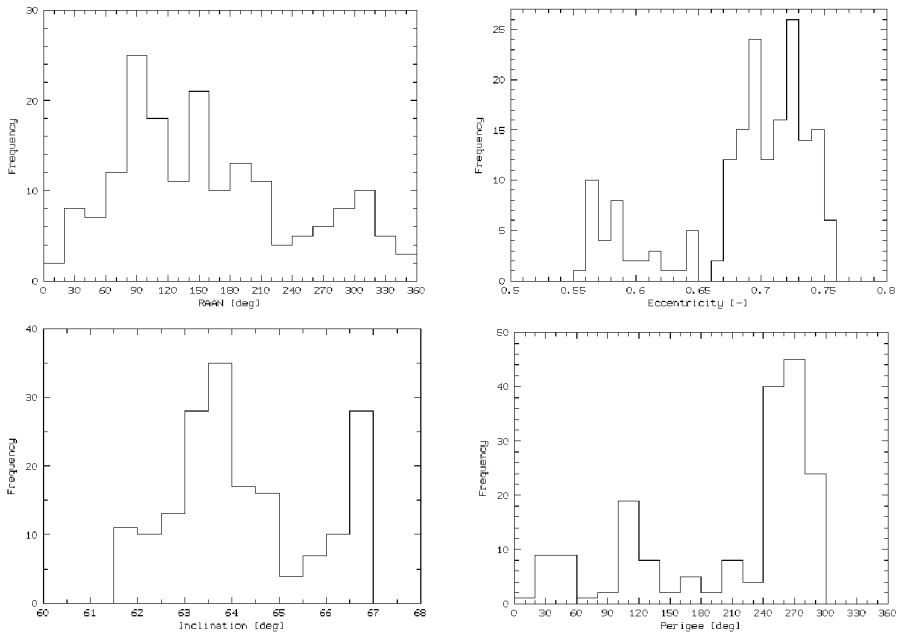

Figure 1: Distribution of four orbital elements of the selected TLE population in January 2012.

Objects in Molniya orbits are vey difficult to observe optically around the perigee due to visibility constraints and the high angular velocities. The selected TLE population includes 55 objects with a perigee between 0° and 180°, i.e. above the northern hemisphere. About half of them have their perigee around 90°. Objects with a perigee of less than 180° are rocket bodies (16), debris (32) and OKO satellites (7).

Figure 2 shows the geocentric passes in the RA/DE system of the selected TLE population as seen from the OGS during one night in January 2012. There is a region with enhanced apparent density in the declination stripe around 63°. In this culmination region most of the objects, namely the objects whose orbits have an argument of perigee around -90°, reach their apogee.

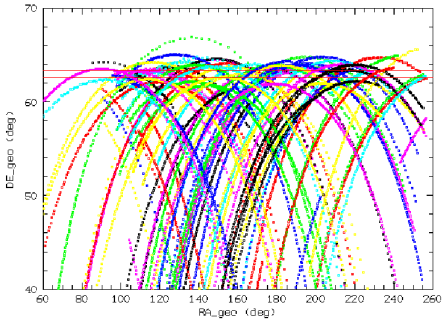

Figure 2: Geocentric passes in the RA/DE system of the selected population seen from the OGS during one night in January 2012.

Since implementing an efficient detection strategy requires the optimization of the tracking rates and the integration time, we look for regions where the changes in apparent velocity are small. Figure 3 shows the topocentric angular velocities in RA/DE system as a function of declination seen from the OGS. The minimal angular velocity is around 7''/s for objects with a declination between 60° and 70°. Objects with a perigee around 90° reach their minimal angular velocity at a declination between -30° and -40°.

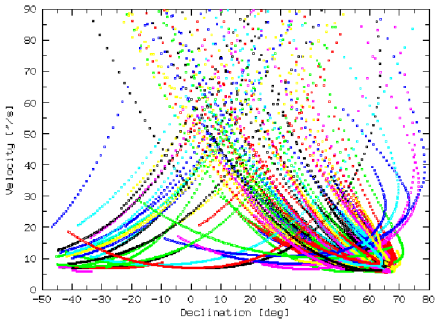

Figure 3: Topocentric angular velocities as a function of DE seen from the OGS.

The velocity decreases with increasing distance. But a bigger distance results in fainter apparent magnitudes. On the other hand the detection limit also depends on the illumination of the observed objects and in particular on the phase angle. Figure 4 shows the phase angle for small angular velocities as a function of the angular velocity. The phase angles range from about 40° to 100°.

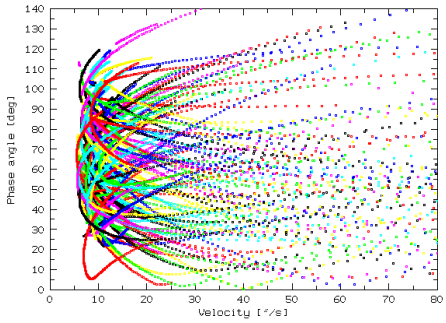

Figure 4: Angular velocity as a function of phase angle.

3 EVOLUTION OF THE ORBITAL ELEMENTS

Using the selected TLE population, simulations have been performed to analyze the evolution of the orbital elements. For this propagation a full force model was used including the gravitational attraction of the Sun and the Moon. Further Earth's potential coefficients up to terms of degree and order 12, the perturbations due to the Earth tides, the corrections due to general relativity, and a simple model for the direct radiation pressure including eclipses by the Earth were included [3]. An AMR value of 0.009 kg/m^2 both, for air drag and radiation pressure, was used. The drag coefficient cD was fixed at two.

The daily drift of the nodes for the analyzed TLE population is about -0.1° to -0.2°/day which corresponds to a drift of about -35° to -70°/year. Most of the objects keep their eccentricity and inclination over the simulated time interval whereas objects with an initial eccentricity of less than 0.65 and an inclination of more than 65° change the inclination and the perigee. An inclination of more than 63.4° (critical inclination) caused a negative drift of the perigee. Therefore the perigee of these objects drift to lower values during the simulated 20 years. The eccentricity is slightly increasing. Finally some objects re-entered during the simulated 20 years.

A comparison of the distributions of the orbital elements of the current population with the distributions of the orbital elements 20 years later (Figure 5) shows no fundamental differences. Because of the drift of the nodes the maxima in Figure 5 are shifted. During the simulations more than 40% of the objects were lost because they re-entered in the atmosphere. Taking into account that the oldest objects are in orbit since about 30 years we can expect that the current distribution still essentially represents the initial distribution.

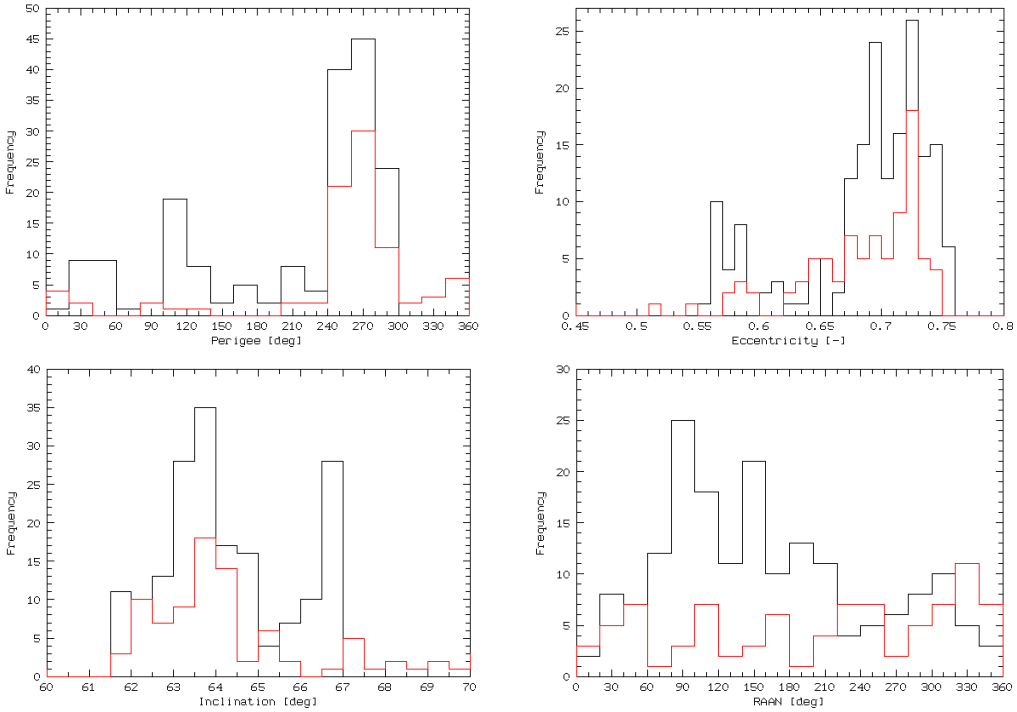

Figure 5: Distributions of four orbital elements of the selected Molniya population in January 2012 (black) and after 20 years (red).

4 SURVEY STRATEGY

Using the ESASDT with a Field of View (FOV) of 0.7x0.7deg^2 a short FOV crossing time can be expected for objects in Molniya orbits. If the maximum angular velocity is about 20"/s a minimum FOV crossing time of 126s and six consecutive observations can be expected for sidereal tracking. However, lower angular velocities are reached at the apogee of the orbit. Most of the objects reach angular velocities of less than 20"/s at declinations higher than 40° (see Figure 3). The minimum angular velocity is about 7"/s.

Next to the angular velocity, the phase angle and the related illumination conditions are important to detect an object. An observation field in anti-sun direction would provide the best illumination conditions. Such a field would also be observable during the whole observation night. With a mean motion of about 2 revolutions per day an uninterrupted observation of 12 hours per field would be the optimum. Such a survey strategy would allow to observe each object in a specific Molniya orbital plane once per night.

Survey observations were performed with the ESASDT at three consecutive nights per month. Each night only one field was selected to be observed. These three fields per month were chosen such that the right ascension of the second field was 180° from the right ascension of the sun. The first and the third field had the same declination but were displaced by 10° in right ascension (see Figure 6).

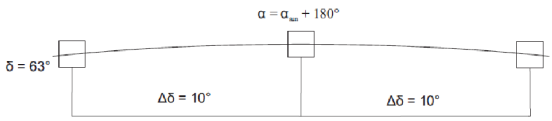

Figure 6: Survey strategy with 3 fields per month displaced by 10 ° in right ascension.

5 OBSERVATIONS AND RESULTS

Observations were performed between January and April 2013. During these four months survey observations were performed at nine nights and at nine different geocentric fields. During one survey a single geocentric field was observed for 10 minutes. If a faint object was found, follow-up observations were performed during the same night to ensure a save rediscovery during the next nights. All observations performed during a single FoV crossing are called tracklet. If there were three or more tracklets of one object during the discovery night, an orbit was determined and this object was scheduled for further observations during the following nights.

Finally 195 surveys were performed during these nine nights corresponding to about 22 surveys per night. In total 24 uncorrelated faint objects were discovered and all known catalogue objects in the survey fields were detected. On average one uncorrelated object was discovered every 80 minutes. Figure 7 shows the perigee as a function of the node for the selected TLE objects (black) and the newly discovered objects (red). Because of the selection of the observations fields, only objects with a RAAN of less than 100° could be found.

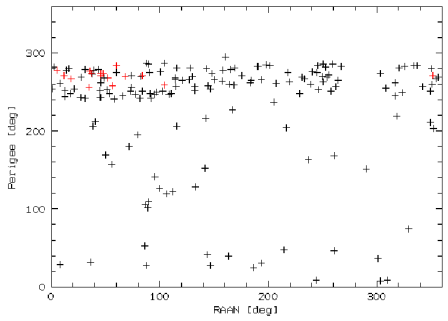

Figure 7: Perigee as a function of the node for the selected TLE population (black) and the newly discovered objects (red).

Figure 8 shows the eccentricity as a function of the inclination for the known objects (black) and the newly discovered objects (red).

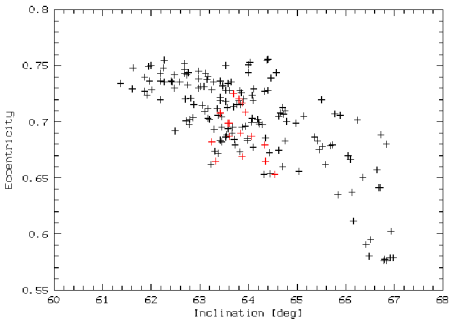

Figure 8: Eccentricity as function of inclination for the selected TLE population (black) and the newly discovered objects (red).

Successful follow-up observations during the night of discovery could be performed for 17 objects. Based on these observations a first orbit was determined and further observations were planned. In the subsequence nights 7 objects could be confirmed by further observations. A distribution of the observed arc length is shown in Figure 9.

For objects with observation arcs of more than one month it is possible to estimate the Area-to-Mass Ratio (AMR) during the orbit determination. A distribution of the estimated AMR values is shown in Table 2. The estimated AMR of three objects is higher than 0.15 what allows to classify these objects as High-Area-to-Mass

objects (HAMR).

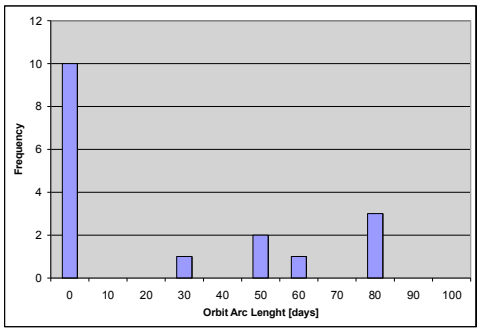

Figure 9: Distribution of the arc length of the observed objects.

Table 2: Estimated AMR values for objects with observed arcs of more than one month.

Objects	AMR [m²/kg]
E13009B	0.24
E13010A	3.59
E13010B	0.17
E13010C	0.07
E13039A	0.02
E13039B	0.04
E13040A	0.0076

The surveys were optimized to discover faint objects. Most of the discovered objects are fainter than 16mag. Figure 10 shows the distribution of the magnitude of the new objects.

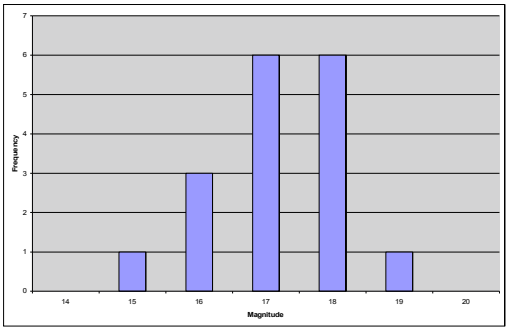

Figure 10: Distribution of magnitude of the discovered objects.

For catalogue maintenance observations of these newly discovered faint objects were also performed with AIUB ´s 1m ZIMLAT telescope in Zimmerwald, Switzerland. Due to the weather conditions only a few observations of these objects could be performed. A short analysis of the variation of the brightness of one object is shown in Figure 11.

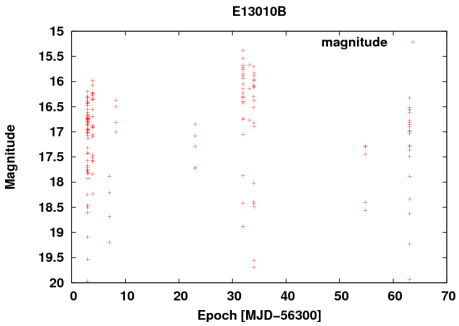

Figure 11: Variation of the magnitude of one discovered object.

6 CONCLUSIONS

The MEO region is sparsely populated and the highest probability for detecting space debris is close to the orbital planes of known objects assuming that the orbital planes of most debris objects are similar to the ones of their parent objects. The analysis of the current TLE population of the Molniya orbit region showed that there are only about 171 known objects in this region. The evolution of the orbital elements shows that the distribution of the orbital elements of the current population is most likely very similar to the initial distribution.

During nine nights about 32 hours of survey observations were performed and 25 uncorrelated objects were discovered. Some of these objects show a considerable brightness variation and have a high AMR. Objects where an orbit was determined were inserted into the AIUB internal catalogue and further observations are planned.

7 REFERENCES

1. Beutler G. (2005). *Methods of Celestial Mechanics*, 2 Volumes. Springer
2. Hinze A., Schildknecht T., Vananti A., Krag H. (2011). *Results from first space debris survey observations in MEO*. European Space Debris Conference, Madrid
3. Schildknecht T., Vananti A., Hinze A., et al. (2011). *Results of optical surveys for Space Debris in MEO*. IAC, Cap Town, IAC-11-A6.1.03
4. Hinze A., Schildknecht T., Vananti A. (2010). *Follow-up Strategies for MEO observations.* 38th Cospar Conference, Bremen
5. Schildknecht T., Flohrer T., Vananti A. (2009). *Optical surveys for Space Debris in MEO – Simulations and First Results*. 60th IAC